ISSN 1063-7788, Physics of Atomic Nuclei, 2026, Vol. 89, No. 3, pp. 267–276. © Pleiades Publishing, Ltd., 2026.

NUCLEI
Experiment

Measurement of Cross Sections for the Nuclear Reactions ^{6}Li$(d,\alpha)^4$He,^{6}Li $(d,p)^7$Li, and ^{6}Li$(d,p)^7$Li* at Deuteron Energies of up to 2.2 MeV

S. Yu. Taskaev[1),2),3)*], M. I. Bikchurina[1),2)], T. A. Bykov[1),2)], D. A. Kasatov[1),2)], Ya. A. Kolesnikov[1),2)], G. M. Ostreinov[1),2)], S. S. Savinov[1),2)], and E. O. Sokolova[1),2)]

Received March 25, 2026; revised April 7, 2026; accepted April 7, 2026

Abstract—The interaction of a deuteron beam with lithium is characterized by a high neutron yield, a high neutron energy, and a wide variety of reactions. The cross sections of the reactions ^{7}Li$(d,n)^8$Be, ^{7}Li $(d,n)^8$Be*, ^{6}Li$(d,\alpha)^4$He, ^{6}Li$(d,p)^7$Li, ^{6}Li$(d,p)^7$Li*, ^{7}Li$(d,\alpha)^5$He, and ^{7}Li $(d,n\alpha)^4$He were measured by our group earlier. In the present study, lithium enriched in the isotope ^{6}Li is used instead of natural lithium, and the cross sections of the reactions ^{6}Li$(d,\alpha)^4$He, ^{6}Li$(d,p)^7$Li, and ^{6}Li$(d,p)^7$Li* are measured here more precisely. The measured cross sections of the reactions ^{6}Li$(d,p)^7$Li and ^{6}Li$(d,p)^7$Li* agree well with our previous measurements up to the deuteron energy of 1.2 MeV but differ from them at deuteron energies above 1.2 MeV.

DOI: 10.1134/S106377882660048X

1. INTRODUCTION

Intense fluxes of fast neutrons are necessary for many applications, including radiation tests of modern materials and equipment. The highest neutron yield is provided by the reaction Li(d,n) at energies starting from 1 MeV [1]. Deuteron interaction with lithium nuclei gives rise to eleven reactions, of which six lead to the production of neutrons. Protons, neutrons, tritium, and alpha particles originate from this interaction along with ^{3}He, ^{5}He, ^{5}Li, ^{7}Li, ^{7}Be, and ^{8}Be nuclei [2]. Of course, knowledge of nuclear-reaction cross sections is of importance for evaluation of nuclear data and the neutron spectrum in radiation tests of materials and for analysis of the possibility of employing lithium as the first wall of a thermonuclear reactor. However, data on reaction cross sections in the literature and databases differ substantially [3–11]; for a number of reactions, there are no data on cross sections. The distinctions between data of different authors are most probably due to the difficulty in determining the thickness of layers of lithium because of its high chemical activity, and this prevents the use of some methods of measurements.

Previously, our group measured the cross sections of the reactions ^{6}Li$(d,\alpha)^4$He, ^{6}Li$(d,p)^7$Li, ^{6}Li$(d,p)^7$Li*, ^{7}Li$(d,\alpha)^5$He, and ^{7}Li$(d,n\alpha)^4$He by means of an alpha spectrometer [12] and the cross sections of the reactions ^{7}Li$(d,n)^8$Be and ^{7}Li$(d,n)^8$Be* by means of the spectrometric fast-neutron radiometer [13]. In those studies, we used natural-lithium layers 1.79 μm thick as a target.

In the present study, we employ lithium enriched in the isotope ^{6}Li. The use of ^{6}Li targets makes it possible to reduce substantially the yield of particles from reactions induced by deuteron interaction with ^{7}Li and characterized by higher production rates and to measure more precisely the cross sections of reactions occurring on ^{6}Li.

The objective of the present study is to carry out a more precise measurement of the cross sections for the reactions ^{6}Li$(d,\alpha)^4$He, ^{6}Li$(d,p)^7$Li and ^{6}Li$(d,p)^7$Li*.

2. EXPERIMENTAL SETUP

The present study was performed using the VITA accelerator neutron source at the Budker Institute of Nuclear Physics, Siberian Branch, Russian Academy of Sciences, in Novosibirsk [1, 14]. The layout of our experimental setup is shown in Fig. 1.

A steady-state monoenergetic deuteron beam is obtained in the VITA vacuum-insulated tandem accelerator (*1*) and is directed to a lithium target (*4*) through a cooled collimator (*3*) 1 mm in diameter situated at a distance of 4 m from the target. The

[1)]Budker Institute of Nuclear Physics, Siberian Branch, Russian Academy of Sciences, Novosibirsk, Russia.
[2)]Novosibirsk State University, Novosibirsk, Russia.
[3)]Joint Institute for Nuclear Research, Dubna, Russia.
[*]E-mail: taskaev@inp.nsk.su

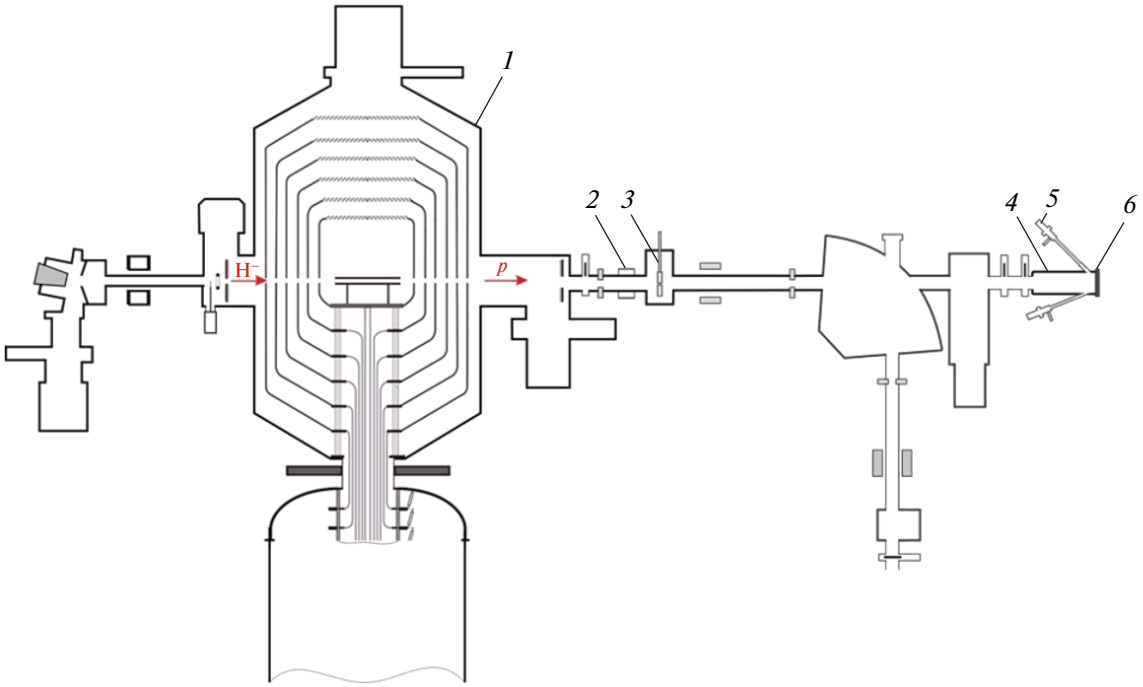


Fig. 1. Layout of the experimental setup: (*1*) vacuum-insulated tandem accelerator, (*2*) DC transformer, (*3*) collimator, (*4*) target unit, (*5*) α-spectrometer, and (*6*) lithium target.

deuteron-beam position and dimensions at the target is monitored by means of the Hikvision camera recording the luminescence of lithium under the effect of deuterons. The deuteron-beam diameter at the surface of the lithium target is 5 mm. The current of the deuteron beam irradiating the lithium target is usually 1 to 2 μA, its minimum and maximum values being 0.4 and 3.7 μA, respectively; the current is stable within 0.4%. One can change the deuteron-beam energy between 0.1 and 2.2 MeV, maintaining its stability at a level of 0.1%.

The deuteron-beam current at the accelerator outlet in front of the collimator is measured and controlled by means of an NPCT (New Parametric Current Transformer, Bergoz Instrumentation, France) *2* nondestructive DC transformer; the magnitude of the current is about 0.5 mA. The deuteron-beam current at the lithium target is measured and controlled using a calibrated resistance connected to a target unit, which is electrically insulated from the setup. Although the target unit is fabricated in the form of deep Faraday cup, electron emission from it is observed at a level of 1% of the ion current [15, 16]. This electron emission increases the ion current by 1%, which is taken into account.

The charged-particle beam obtained in the electrostatic tandem accelerator contains predominantly D^+ ions, but D_2^+ ions and D_0 neutrals are also present in the beam. Ions of D_2 are produced in the ion source together with ions of D, while D_0 neutrals are formed in the gaseous stripping target of the tandem accelerator owing to an incomplete stripping of D^- ions to D^+ ions [1]. It should be noted that D_2^+ ions and D_0 neutrals interact with lithium nuclei as particles of energy one-half as high as the energy of D^+ ions. The contribution of the component whose energy is one-half of the energy of D^+ ions was thoroughly measured earlier, and the results of these measurements were described in detail elsewhere [12]. This contribution amounts to 2%.

A resistance divider connected to a high-voltage electrode of the accelerator is used to measure the energy of protons/deuterons to a precision of 0.1% [15]. The resistive divider is calibrated by means of the threshold reactions ^{7}Li$(p,n)^7$Be and ^{9}Be$(p,n)^9$B.

A thermal vacuum deposition of lithium onto a copper target substrate is carried out at a dedicated test bench. After the deposition of lithium layer, the target unit *4* is covered with a gate valve in order to preserve a vacuum within it, is disconnected from the lithium deposition bench, is transferred to the experimental setup, and is connected to the setup. In the present study, we use lithium enriched in the isotope ^{6}Li and produced at the Novosibirsk Chemical Concentrate Plant.

The intensity and energy of charged particles is measured by an alpha spectrometer (*5* in Fig. 1) based on a silicon spectrometric detector of alpha radiation (PDPA-1K model developed at the Institute for

Physico-Technical Problems, Dubna, Russia). The area of the detector sensitive surface is $S = 20 \pm 1$ mm^2; the detector energy resolution is 13 keV; the energy equivalent of noise is 7 keV; the capacitance is 30 pF; the thickness of the inlet window is 0.08 μm; and a standard natural background lies in the range between 3 and 8 MeV—0.15 pulse/(cm^2 h).

In measuring the cross section, the sensitive part of the alpha spectrometer is positioned at a distance of $R = 585 \pm 1$ mm from the target at an angle of $135 \pm 0.5^\circ$ to the deuteron momentum. The solid angle is $\Omega_{\text{lab}} = S/R^2 = 5.84 \times 10^{-5}$, where $S = 20 \pm 1$ mm^2 (according to the testing certificate of the silicon spectrometric radiation receiver; the identification number is 15264-96). The inaccuracy in measuring the solid angle is determined by the uncertainty in measurement of the area of the spectrometer sensitive part and was found to be 5%.

The alpha-radiation spectrometer was calibrated by means of two reference radiation sources based on the ^{239}Pu nuclide of activity 4.01×10^5 Bq (certificate no. 6887; identification number 7165, 2P9-405.85; production date September 12, 1985) and 1.21×10^5 Bq (certificate no. 6882; identification number 7160, 1P9-105.85; production date September 12, 1985). The fiducial boundaries of the total uncertainty in the results of activity measurement for either source are 19% according to the certificates. The alpha-spectrometer detection efficiency was determined upon placing the reference radiation sources at a distance of 102.8 mm from the detector surface and measuring their activity. The measured activities of the sources were 4.16×10^5 and 1.22×10^5 Bq, which are higher than the certificate values by, respectively, 4 and 1.5%, but which comply with them within the uncertainties. Since the measured source activities agree with certificate values and since the reference radiation sources are independent, the calibration confirms the assumption that the detector in question records alpha particles with an efficiency of 100%; that is, $k = 1$.

The calibration of the spectrometer in energy was performed using a reference spectrometric α-source of activity 3.84×10^4 Bq based on the isotope ^{226}Ra (certificate no. 425/331/10692-A of October 21, 1977). The energies of alpha particles from dominant transitions are 4601, 4784.3, 5304.3, 5489.5, 6002.55, and 7686.82 keV [17]. It is found that the dependence of the energy E on the channel number N is described by the linear expression $E\,[\text{keV}] = 1.3904N + 96.734$, the confidence level of the approximation being $R^2 = 0.99998$.

3. NUCLEAR REACTIONS

Deuteron interaction with a lithium nucleus at deuteron energies below 2.2 MeV leads to the following nucleus reactions [2]:

$$^7\text{Li} + d = n + {}^8\text{Be} + 15.028\ \text{MeV},$$
$$^8\text{Be} \to 2\alpha + 0.094\ \text{MeV}; \quad (1)$$
$$^7\text{Li} + d = n + {}^8\text{Be}^* + 12.148\ \text{MeV},$$
$$^8\text{Be}^* \to 2\alpha + 2.974\ \text{MeV}; \quad (2)$$
$$^7\text{Li} + d = n + \alpha + \alpha + 15.121\ \text{MeV}; \quad (3)$$
$$^7\text{Li} + d = \alpha + {}^5\text{He} + 14.162\ \text{MeV},$$
$$^5\text{He} \to n + \alpha + 0.957\ \text{MeV}; \quad (4)$$
$$^6\text{Li} + d = \alpha + \alpha + 22.38\ \text{MeV}; \quad (5)$$
$$^6\text{Li} + d = n + {}^7\text{Be} + 3.385\ \text{MeV}; \quad (6)$$
$$^6\text{Li} + d = p + {}^7\text{Li} + 5.028\ \text{MeV}; \quad (7)$$
$$^6\text{Li} + d = p + {}^7\text{Li}^* + 4.550\ \text{MeV}; \quad (8)$$
$$^6\text{Li} + d = t + p + \alpha + 2.6\ \text{MeV}; \quad (9)$$
$$^6\text{Li} + d = t + {}^5\text{Li} + 0.595\ \text{MeV},$$
$$^5\text{Li} \to \alpha + p + 1.965\ \text{MeV}; \quad (10)$$
$$^6\text{Li} + d = {}^3\text{He} + {}^5\text{He} + 0.840\ \text{MeV},$$
$$^5\text{He} \to n + \alpha + 0.957\ \text{MeV}. \quad (11)$$

Previously, we measured the cross section for the reactions in Eqs. (1)–(5), (7), and (8)—namely, for the reactions $^7\text{Li}(d,n)^8\text{Be}$, $^7\text{Li}(d,n)^8\text{Be}^*$, $^7\text{Li}(d,n\alpha)^4\text{He}$, $^7\text{Li}(d,\alpha)^5\text{He}$, $^6\text{Li}(d,\alpha)^4\text{He}$, $^6\text{Li}(d,p)^7\text{Li}$, and $^6\text{Li}(d,p)^7\text{Li}^*$ [13, 14]. The objective of the present study is to measure more precisely the cross sections of the reactions $^6\text{Li}(d,\alpha)^4\text{He}$, $^6\text{Li}(d,p)^7\text{Li}$, and $^6\text{Li}(d,p)^7\text{Li}^*$, employing a lithium target enriched in the isotope ^{6}Li.

4. METHODOLOGY OF DETERMINATION OF CROSS SECTIONS

The differential reaction cross section (in cm^2/sr units) in the laboratory frame, $d\sigma/d\Omega$, is determined by the formula $\frac{d\sigma}{d\Omega} = \frac{eY}{N\,k\,n\,l\,\Phi\,\Omega_{\text{lab}}}$, where e is an elementary charge [Coulomb (C) units], Y is the measured particle yield (integral under the peak), N is the number of measured charged particles in a specific reaction ($N = 2$ in the reaction $^6\text{Li}(d,\alpha)^4\text{He}$ and $N = 1$ in the reactions $^6\text{Li}(d,p)^7\text{Li}$ and $^6\text{Li}(d,p)^7\text{Li}^*$), k is the particle-detection efficiency of the spectrometer, n is the density of lithium nuclei [in cm^{-3}], l is the lithium-layer thickness (in centimeters), Φ is the fluence of D^+ ions (in mC units), and Ω_{lab} is the solid angle.

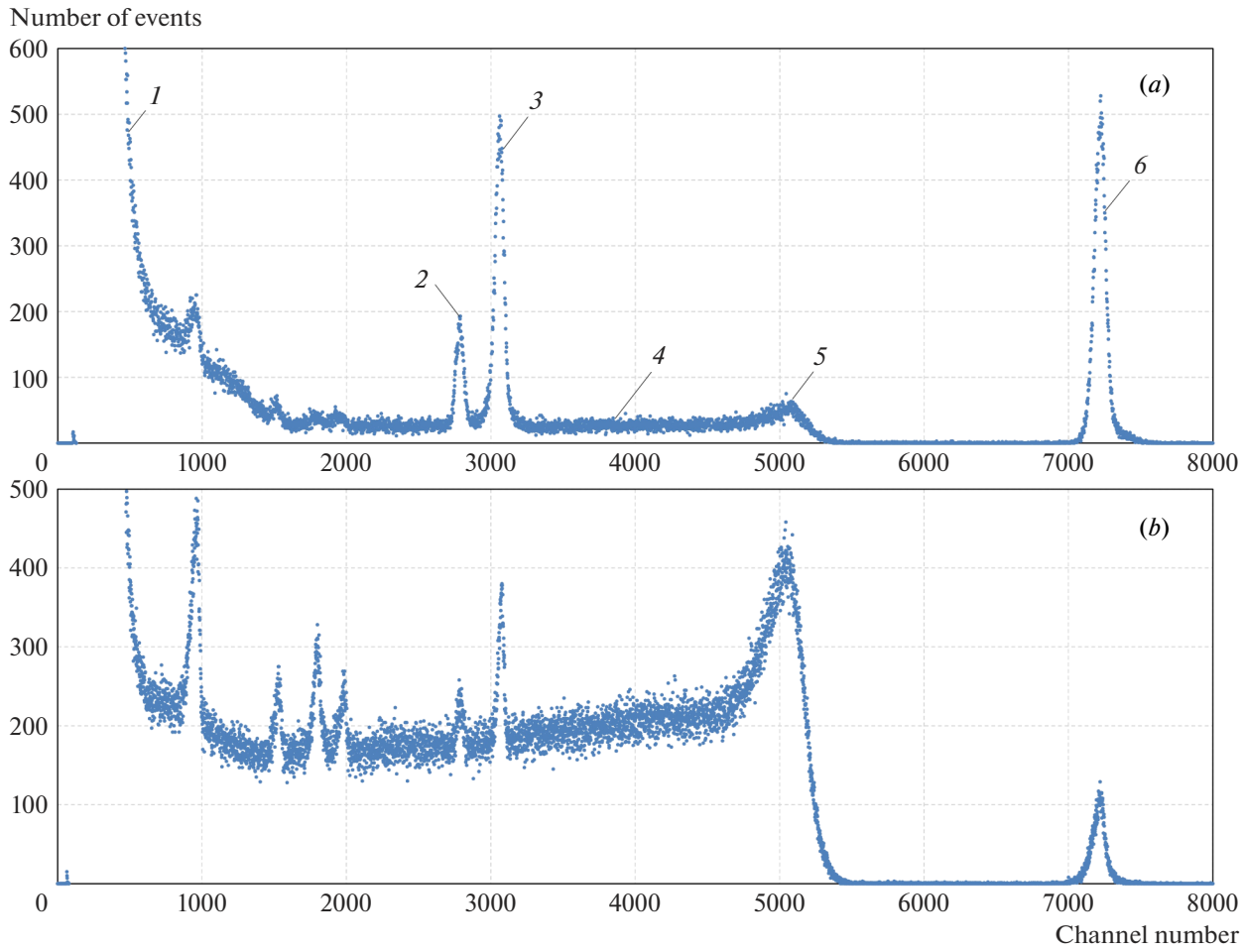


Fig. 2. Signal of the α-spectrometer at the deuteron-beam energy of 0.6 MeV in the cases of targets from (*a*) lithium enriched in the isotope ^{6}Li and (*b*) lithium of natural isotopic composition: (*1*) backscattered deuterons, (*2*) protons from the reaction $^6\mathrm{Li}(d,p)^7\mathrm{Li}^*$, (*3*) protons from the reaction $^6\mathrm{Li}(d,p)^7\mathrm{Li}$, (*4*) alpha particles from the reaction $^7\mathrm{Li}(d,n\alpha)^4\mathrm{He}$, (*5*) alpha particles from the reaction $^7\mathrm{Li}(d,\alpha)^5\mathrm{He}$, and (*6*) alpha particles from the reaction $^6\mathrm{Li}(d,\alpha)^4\mathrm{He}$.

5. RESULTS AND DISCUSSION

The characteristic energy spectrum of charged particles detected by the alpha spectrometer is shown in Fig. 2*a*. The left-hand part of the graph is dominated by a signal from backward-scattered deuterons (*1*), which includes binary and ternary events. Peaks *2* and *3* are associated with protons from the reactions $^6\mathrm{Li}(d,p)^7\mathrm{Li}^*$ and $^6\mathrm{Li}(d,p)^7\mathrm{Li}$, respectively. A wide plateau (*4*) and a broadened peak (*5*) correspond to alpha particles from the reactions $^7\mathrm{Li}(d,n\alpha)^4\mathrm{He}$ and $^7\mathrm{Li}(d,\alpha)^5\mathrm{He}$. Peak *6* is formed by alpha particles from the reaction$^6\mathrm{Li}(d,\alpha)^4\mathrm{He}$.

The signal that we obtained earlier under the analogous conditions but with a target from natural lithium [12] is shown in Fig. 2*b* for the sake of comparison. One can see that the use of lithium enriched in the isotope ^{6}Li increases the particle-production rate in the reactions involving ^{6}Li against a decrease in the production rate in the reactions involving ^{7}Li.

Two alpha particles of equally high energy are produced in the reaction $^6\mathrm{Li}(d,\alpha)^4\mathrm{He}$; therefore, the alpha particles are readily identified in the measured energy spectrum of charged particles (see peak *6* in Fig. 1). This alpha-particle peak is rather far off the other detected events, so that one can easily determine the integral under this peak.

The measured yields of alpha particles and protons (integral under the peak), Y, in the reactions $^6\mathrm{Li}(d,\alpha)^4\mathrm{He}$, $^6\mathrm{Li}(d,p)^7\mathrm{Li}$, and $^6\mathrm{Li}(d,p)^7\mathrm{Li}^*$ at a detection angle of 135° are given in Table 1. The measurements were performed with a step of 100 keV in the deuteron-beam energy. The stability of the measured energy was 1 to 2 keV, the maximum value being 3.2 keV.

In employing a target from natural lithium, its thickness was measured by six independent methods

Table 1. Parameters of measurements: deuteron energy (E); stability of deuteron energy (ΔE); total and live time of measurements with the aid of the alpha spectrometer (T_{total} and T_{live}); fluence of D^+ ions (L); and experimental charged-particle yield (Y), which is determined as the integral under the peak

E, keV	ΔE, keV	T_{total}, s	T_{live}, s	Φ, mC	Y, events		
					$^6\text{Li}(d,\alpha)^4\text{He}$	$^6\text{Li}(d,p)^7\text{Li}$	$^6\text{Li}(d,p)^7\text{Li}^*$
200.8	0.8	1423.37	1423.35	0.64	288	175	41
301.3	0.9	1296.23	1295.61	1.80	4589	2592	592
401.3	0.9	1309.05	1304.26	4.02	21 256	12 822	3096
502.0	1.0	1201.98	1192.68	4.38	31 882	20 712	5440
599.6	1.5	1206.49	1192.60	3.95	31 912	22 473	6327
650.9	1.3	4249.80	4183.65	8.30	67 873	51 519	15 791
700.5	1.2	1233.02	1204.34	2.57	20 858	16 160	5250
800.4	1.4	1241.52	1206.08	2.26	17 607	14 641	5174
900.4	1.8	1256.80	1210.59	2.47	18 099	15 462	5901
1003.1	1.6	1249.88	1195.39	2.61	18 110	16 825	6808
1100.9	1.3	1234.67	1178.06	2.54	16 302	15 573	7152
1201.6	1.4	1263.15	1193.03	3.03	18 154	17 039	8362
1301.4	1.4	1213.50	1175.35	1.55	8672	7868	4898
1402.2	1.4	1261.04	1217.23	1.76	9550	8489	6307
1499.7	2.8	1249.60	1211.37	1.52	7725	6667	5672
1600.4	1.6	1245.20	1200.89	1.77	8379	6405	6402
1700.3	1.6	1234.86	1189.33	1.80	8256	6406	6792
1800.7	1.6	1227.07	1181.86	1.84	7711	6430	6272
1901.0	2.4	1236.75	1186.02	2.05	8628	6319	6993
2001.5	2.2	1240.65	1197.36	1.73	7405	4893	5006
2101.5	1.7	1250.33	1208.15	1.66	6877	4097	4505
2202.0	3.2	1236.91	1199.78	1.48	5798	2867	3481

and was found to be 1.79 ± 0.07 μm [12]. The most precise measurement of the lithium-target thickness was performed using a new in situ method [18, 19]. The method is based on comparing the yield of 478-keV photons in the reaction $^7\text{Li}(p,p'\gamma)^7\text{Li}$ from the lithium layer under study and a thick lithium layer that are irradiated with a proton beam. In our previous investigation, we employed natural lithium produced at the Novosibirsk Chemical Concentrate Plant; the concentration of lithium in the sample used was 99.956%. The concentration of ^{7}Li in natural lithium ranges between 92.41% [20] and 92.58% [21]; we took its average value of 92.5%. For the ensuing analysis, we introduce the concepts of the ^{6}Li and ^{7}Li lithium thicknesses; they are 0.134 and 1.656 μm, respectively.

In the present study, the most precise in situ method for determining the lithium-layer thickness is inapplicable, since the isotopic composition of lithium is unknown, the concentration of ^{7}Li being low. The ^{6}Li layer thickness was determined on the basis of a comparison of the differential cross section measured in the present study for the reaction $^6\text{Li}(d,\alpha)^4\text{He}$ and its counterpart measured earlier in [12]. Figure 3 illustrates a comparison of these cross sections under the assumption that the ^{6}Li layer thickness in the target used is 0.963 μm. The least-squares fit led to a minimum value at the ^{6}Li layer thickness of 6 0.963 μm.

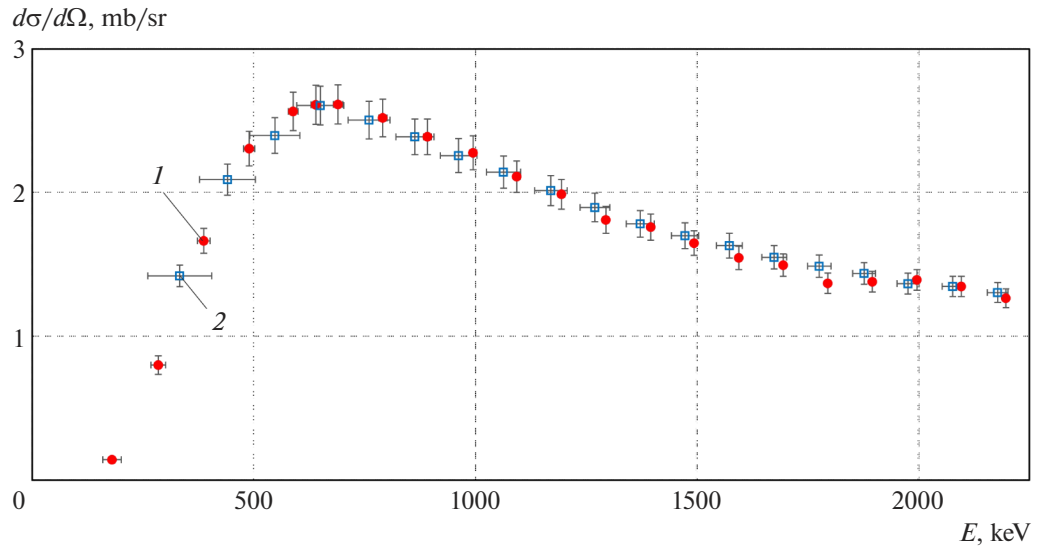


Fig. 3. (*1*) Differential cross section measured for the reaction ^{6}Li$(d,\alpha)^4$He at 135° under the assumption that the ^{6}Li thickness is 0.963 μm along with (*2*) the respective cross section taken from [12] and presented here for the sake of comparison.

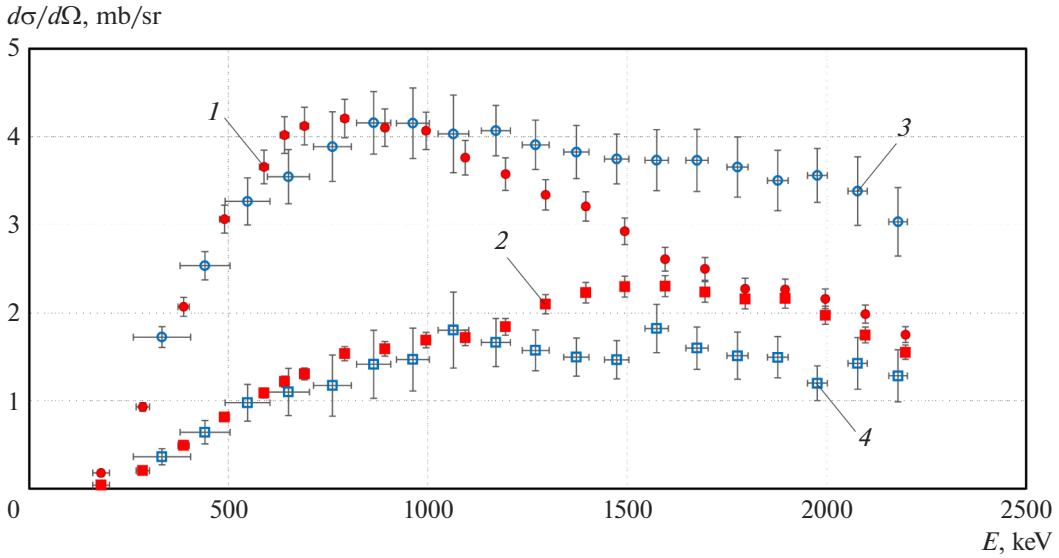


Fig. 4. Measured differential cross sections of the reactions (*1*) ^{6}Li$(d,p)^7$Li and (*2*) ^{6}Li$(d,p)^7$Li* at 135° along with the cross sections of the reactions (*3*) ^{6}Li$(d,p)^7$Li and (*4* ^{6}Li$(d,p)^7$Li* from [12].

The validity of this approach is based on two factors. First, high-energy alpha particles produced in this reaction are readily and reliably identifiable (see peak *6* in Fig. 2). Second, the cross section that we measured earlier for the reaction ^{6}Li$(d,\alpha)^4$He agrees well with the cross section presented in the ENDF/B-VIII.0 library of nuclear reactions [22].

Figure 3 shows that the new and previous values of the differential reaction cross section at the deuteron energy of 0.9 MeV are nearly identical: 2.389 mb/sr in the present experiment versus 2.390 mb/sr in the earlier one. For this example, we will show how we determine the lithium-layer thickness. Since we perform a comparison, we can exclude identical quantities (e, N, k and n) in the expression $\frac{d\sigma}{d\Omega} = \frac{eY}{N\,k\,n\,l\,\Phi\,\Omega_{\text{lab}}}$, reduce it to the form $\frac{d\sigma}{d\Omega} \sim \frac{Y}{l\,\Phi\,\Omega_{\text{lab}}}$, and determine the lithium-layer thickness as l $\frac{Y}{\Phi\,\Omega_{\text{lab}}\,d\sigma/d\Omega}$. In the case being considered, the experimental alpha-particle yield Y became higher by a factor of 1.569

(18099 instead of 11539), the solid angle Ω_{lab} became larger by a factor of 1.523 (5.84×10^{-5} instead of 3.84×10^{-5}), the ion fluence Φ became smaller by a factor of 7.11 (2.419 instead of 17.2 mC), and the differential reaction cross section became smaller by factor of 1.00038 (2.389 instead of 2.390 mb/sr). It follows that the ^{6}Li thickness became larger by a factor of 6.963: 0.963 instead 0.134 μm.

We will determine the ^{7}Li thickness in the following way. Figure 2*a* shows that the intensity of alpha particles in the reaction $^6\mathrm{Li}(d,\alpha)^4\mathrm{He}$ (integral under the peak) is higher than the intensity of alpha particles in the reaction $^7\mathrm{Li}(d,\alpha)^5\mathrm{He}$, but the relationship between the respective intensities in the earlier experiment was opposite (Fig. 2*b*). These intensity values were compared at all values of the deuteron-beam energy from 0.4 MeV to 2.2 MeV, and it was found that the intensity of the signal from ^{7}Li decreased by a factor of 41.2 ± 1.4 in relation to the signal from ^{6}Li. Part of this decrease is due to the increase in the ^{6}Li thickness by a factor of 6.963. This means that the remaining part, that is, 5.917, is due to a decrease in the ^{7}Li thickness. Thus, the ^{7}Li thickness became 0.280 instead of 1.656 μm.

Thus, we found that the lithium-layer thickness is 1.243 ± 0.053 μm, in which ^{6}Li and ^{7}Li exhaust 0.963 ± 0.038 and 0.280 ± 0.015 μm, respectively. The inaccuracy in determining the ^{6}Li thickness is 4%, since it is determined exclusively by the uncertainty in the natural-lithium thickness found earlier. The comparison of the cross sections introduced virtually no uncertainty. The inaccuracy in determining the ^{7}Li thickness increased to 5.2% because of an additional uncertainty in the comparison of the production rates of the reactions $^6\mathrm{Li}(d,\alpha)^4\mathrm{He}$ and $^7\mathrm{Li}(d,\alpha)^5\mathrm{He}$. The inaccuracy in determining the total lithium thickness is 4.2%.

The data that we obtained make it possible to determine the differential cross section for the reaction $^6\mathrm{Li}(d,\alpha)^4\mathrm{He}$; we present it in Fig. 3 and in Table 2. The inaccuracy of the cross-section measurement receives contributions from the uncertainties in determining the ^{6}Li thickness (4%), the efficiency of charged-particle detection (3%), and the density of lithium nuclei Li (1%) and from the standard error (1% in most cases), amounting to 5.2%.

A deuteron traversing a lithium layer 1.243 μm thick loses an energy of 9.1 to 41.6 keV at the energies of, respectively, 2.2 MeV at 0.2 MeV [23]. Table 2 gives the average energy of deuterons in the lithium layer but not the incident-deuteron energy at the lithium surface.

The reactions $^6\mathrm{Li}(d,p)^7\mathrm{Li}$ and $^6\mathrm{Li}(d,p)^7\mathrm{Li}^*$ produce protons detected by the alpha spectrometer (peaks *2* and *3* in Fig. 2). These peaks are clearly identifiable against the plateau associated with alpha particles from the reaction $^7\mathrm{Li}(d,n\alpha)^4\mathrm{He}$ (plateau *4* in Fig. 2). Table 1 gives the measured proton yields (integral under the peak) Y of the reactions

Table 2. Differential cross section σ of the reaction $^6\mathrm{Li}(d,\alpha)^4\mathrm{He}$ at 135° for various values of the deuteron energy E (here, ΔE is the standard deviation of E, while $\Delta\sigma$ is the statistical dispersion of σ)

E, keV	ΔE, keV	σ, mb/sr	$\Delta\sigma$, mb/dr
180	21	0.14	0.01
285	17	0.80	0.06
387	14	1.67	0.09
490	13	2.31	0.12
589	11	2.57	0.13
640	11	2.61	0.14
690	10	2.61	0.14
791	9	2.52	0.13
892	9	2.39	0.12
995	8	2.28	0.12
1093	8	2.11	0.11
1194	7	1.99	0.10
1295	7	1.81	0.09
1396	6	1.76	0.09
1494	6	1.65	0.09
1595	6	1.55	0.08
1695	6	1.50	0.08
1795	5	1.37	0.07
1896	5	1.38	0.07
1997	5	1.39	0.07
2097	5	1.35	0.07
2197	5	1.27	0.07

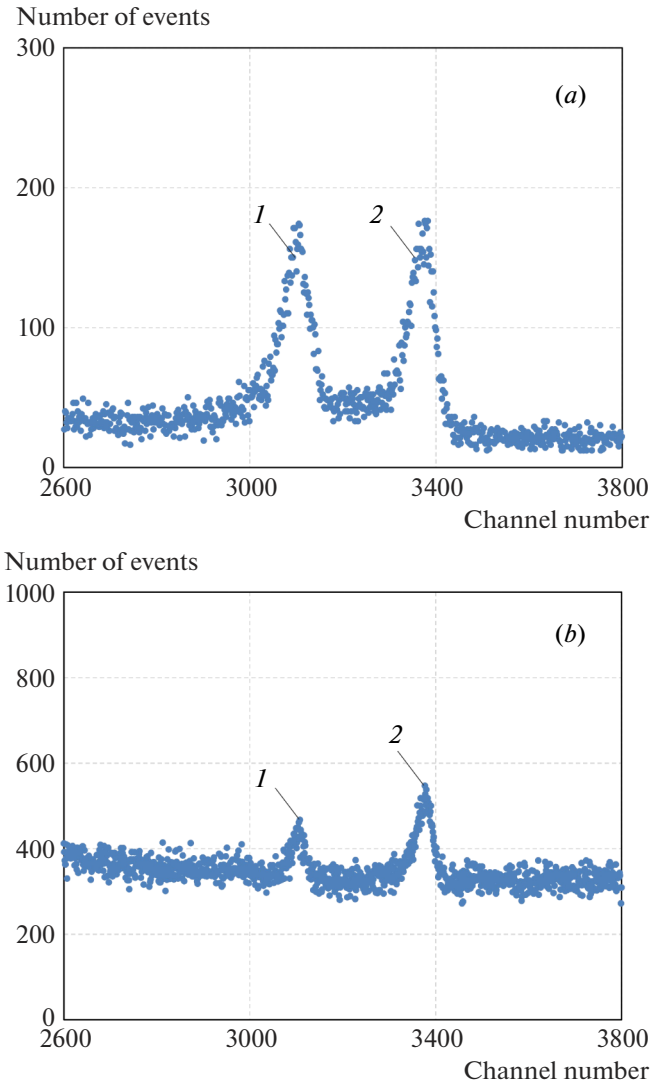


Fig. 5. Signal of the α-spectrometer at the deuteron energy of 1.9 MeV in the cases of targets from (*a*) lithium enriched in the isotope ^{6}Li and (*b*) lithium of natural isotopic composition: (*1*) protons from the reaction $^6\mathrm{Li}(d,p)^7\mathrm{Li}^*$ and (*2*) protons from the reaction $^6\mathrm{Li}(d,p)^7\mathrm{Li}$.

$^6\mathrm{Li}(d,p)^7\mathrm{Li}$ and $^6\mathrm{Li}(d,p)^7\mathrm{Li}^*$ at 135°. The data that we obtained make it possible to determine the differential cross section for the reactions $^6\mathrm{Li}(d,p)^7\mathrm{Li}$ and $^6\mathrm{Li}(d,p)^7\mathrm{Li}^*$ (Fig. 4 and Table 3).

The inaccuracy of the cross-section measurement is associated with the uncertainties in determining the ^{7}Li thickness (5.2%), the efficiency of charged-particle detection (3%), and the density of lithium nuclei (1%). Previously, the measurement error received a dominant contribution from the inaccuracy in the measurement of the plateau associated with the reaction $^7\mathrm{Li}(d,n\alpha)^4\mathrm{He}$ and was 5 to 10% for the reaction $^6\mathrm{Li}(d,p)^7\mathrm{Li}$ and 15 to 40% for the reaction $^6\mathrm{Li}(d,p)^7\mathrm{Li}^*$. The respective error now became negligible because of a nearly sevenfold growth of the production rate of the reactions being studied in response to an increase in the ^{6}Li thickness and because of a nearly sixfold reduction of the plateau in response to a decrease in the ^{7}Li thickness. As a result, the ultimate error in the cross-section measurement decreased to 6%.

Figure 4 shows that, at deuteron energies of up to 1.2 MeV, the cross sections measured in the present study for the reactions $^6\mathrm{Li}(d,p)^7\mathrm{Li}$ and $^6\mathrm{Li}(d,p)^7\mathrm{Li}^*$ agree well with those that we measured earlier, but they differ substantially at deuteron energies above 1.2 MeV. We do not know why this occurred. We made use of the same accelerator, the same target, and the same alpha spectrometer. The only difference is that, in the present study, we employ a lithium target 1.243 μm thick enriched in the isotope ^{6}Li, while, previously, we took 1.79-μm-thick layer from lithium of natural isotopic composition.

Figure 2 shows that, at the deuteron energy of 0.6 MeV, the production rate of the reaction $^6\mathrm{Li}(d,p)^7\mathrm{Li}$ is as before higher than the production rate of the reaction $^6\mathrm{Li}(d,p)^7\mathrm{Li}^*$ by a factor of 3.5, but that, at the deuteron energy of 1.9 MeV, the production rates of these reactions are nearly identical (compare peaks *1* and *2* in Fig. 5*a*), whereas, previously, they differed substantially (compare peaks *1* and *2* in Fig. 5*b*). Presently, we are unable to explain this effect.

6. CONCLUSIONS

In our earlier experiment, we measured the cross sections of the nuclear reactions $^6\mathrm{Li}(d,\alpha)^4\mathrm{He}$, $^6\mathrm{Li}(d,p)^7\mathrm{Li}$, $^6\mathrm{Li}(d,p)^7\mathrm{Li}^*$, $^7\mathrm{Li}(d,\alpha)^5\mathrm{He}$, and $^7\mathrm{Li}(d,n\alpha)^4\mathrm{He}$ by applying an alpha spectrometer and the cross sections of the nuclear reactions $^7\mathrm{Li}(d,n)^8\mathrm{Be}$ and $^7\mathrm{Li}(d,n)^8\mathrm{Be}^*$ by applying a spectrometric fast-neutron radiometer. In the present study, we have made use of lithium enriched in the isotope ^{6}Li and have substantially reduced the yield of particles in deuteron interaction with ^{7}Li. This has made it possible to measure more precisely the cross sections of the reactions $^6\mathrm{Li}(d,\alpha)^4\mathrm{He}$, $^6\mathrm{Li}(d,p)^7\mathrm{Li}$, and $^6\mathrm{Li}(d,p)^7\mathrm{Li}^*$. The data that we have obtained are presented in a tabular form. It is worthy of special note that the cross sections measured here for the reactions $^6\mathrm{Li}(d,p)^7\mathrm{Li}$ and $^6\mathrm{Li}(d,p)^7\mathrm{Li}^*$ and those that were measured for these reactions earlier agree well at deuteron energies of up to 1.2 MeV, but that they differ at deuteron energies above 1.2 MeV. The only difference is that, in the present study, we make use of a 1.243-μm-thick layer of lithium enriched in the

Table 3. Differential cross section σ for the reactions ^{6}Li$(d,p)^7$Li and ^{6}Li$(d,p)^7$Li* at 135° for various values of the deuteron energy E (here, ΔE is the standard deviation of E, while $\Delta\sigma$ is the statistical dispersion of σ)

E, keV	ΔE, keV	$\Delta\sigma$, mb/sr	$\Delta\sigma$, mb/sr	$\Delta\sigma$, mb/sr	$\Delta\sigma$, mb/sr
		^{6}Li$(d,p)^7$Li		^{6}Li$(d,p)^7$Li*	
180	21	0.18	0.01	0.04	0.002
285	17	0.93	0.05	0.21	0.01
387	14	2.07	0.11	0.49	0.03
490	13	3.06	0.16	0.82	0.04
589	11	3.66	0.19	1.09	0.06
640	11	4.02	0.21	1.22	0.06
690	10	4.12	0.21	1.31	0.07
791	9	4.21	0.22	1.54	0.08
892	9	4.10	0.21	1.59	0.08
995	8	4.07	0.21	1.69	0.09
1093	8	3.76	0.20	1.72	0.09
1194	7	3.58	0.19	1.84	0.10
1295	7	3.34	0.17	2.10	0.11
1396	6	3.21	0.17	2.23	0.11
1494	6	2.93	0.15	2.30	0.12
1595	6	2.61	0.14	2.30	0.12
1695	6	2.50	0.13	2.24	0.12
1795	5	2.27	0.12	2.16	0.11
1896	5	2.26	0.11	2.17	0.11
1997	5	2.16	0.11	1.97	0.10
2097	5	1.99	0.10	1.75	0.09
2197	5	1.75	0.09	1.55	0.08

isotope ^{6}Li, while, in the previous study, we employed a layer of natural lithium 1.79 μm in thickness. We have no explanation for this effect.

FUNDING

This study was supported by Russian Science Foundation (grant no. 19-72-30005, https://rscf.ru/project/19-72-30005/).

CONFLICT OF INTEREST

The authors of this work declare that they have no conflicts of interest.

REFERENCES

1. S. Yu. Taskaev, *VITA Accelerator-Based Neutron Source* (Fizmatlit, Moskva, 2024).
2. *Tables of Physical Constants, Handbook*, Ed. by I. K. Kikoin (Atomizdat, Moscow, 1976).
3. A. J. Elwyn, R. E. Holland, C. N. Davids, L. Meyer-Schutzmeister, J. E. Monahan, F. P. Mooring, and W. Ray, Phys. Rev. C **16**, 1744 (1977). https://doi.org/10.1103/physrevc.16.1744
4. P. Paul and K. P. Lieb, Nuclear Physics **53**, 465 (1964). https://doi.org/10.1016/0029-5582(64)90626-1
5. F. Bertrand, G. Grenier, and J. Pornet, Rept. Centre d'Etudes Nucleaires, Saclay Reports No. 3428 (1968).
6. J. M. Delbrouck-Habaru, P. D. Dumont, M. Huez, G. Robaye, and L. Winand, Bull. Soc. Roy. Sci. Liege **38**, 240 (1969).

7. V. Foteinou, A. Lagoyannis, M. Kokkoris, G. Provatas, T. Konstantinopoulos, P. Misaelides, and S. Harissopulos, Nucl. Instrum. Methods Phys. Res., Sect. B **269**, 2990 (2011). https://doi.org/10.1016/j.nimb.2011.04.058
8. B. Maurel, G. Amsel, and D. Dieumegard, Nucl. Instrum. Methods Phys. Res. **191**, 349 (1981). https://doi.org/10.1016/0029-554x(81)91028-4
9. G. Bruno, J. Decharge, A. Perrin, G. Surget, and C. Thibault, J. Phys. (France) **27**, 517 (1966).
10. W. Whaling and T. W. Bonner, Phys. Rev. **79**, 258 (1950). https://doi.org/10.1103/physrev.79.258
11. F. Hirst, I. Johnstone, and M. J. Poole, The London Edinburgh and Dublin Philosophical Magazine and Journal of Science **45**, 762 (1954).
12. S. Taskaev, M. Bikchurina, T. Bykov, D. Kasatov, I. Kolesnikov, G. Ostreinov, S. Savinov, and E. Sokolova, Nucl. Instrum. Methods Phys. Res., Sect. B **554**, 165460 (2024). https://doi.org/10.1016/j.nimb.2024.165460
13. S. A. Meshchaninov, A. V. Krasilnikov, N. B. Rodionov, Yu. A. Kashchuk, S. Yu. Obudovsky, A. S. Dzhurik, T. M. Kormilitsyn, R. N. Rodionov, V. N. Amosov, G. E. Nemtsev, M. I. Bikchurina, T. A. Bykov, G. D. Verkhovod, D. A. Kasatov, Ya. A. Kolesnikov, G. M. Ostreinov, E. O. Sokolova, and S. Yu. Taskaev, Phys. At. Nucl. **87**, 769 (2024). https://doi.org/10.1134/s1063778824700789
14. S. Taskaev, E. Berendeev, M. Bikchurina, T. Bykov, D. Kasatov, I. Kolesnikov, A. Koshkarev, A. Makarov, G. Ostreinov, V. Porosev, S. Savinov, I. Shchudlo, E. Sokolova, I. Sorokin, T. Sycheva, and G. Verkhovod, Biology **10**, 350 (2021). https://doi.org/10.3390/biology10050350
15. M. Bikchurina, T. Bykov, D. Kasatov, I. Kolesnikov, A. Makarov, I. Shchudlo, E. Sokolova, and S. Taskaev, Biology **10**, 824 (2021). https://doi.org/10.3390/biology10090824
16. M. I. Bikchurina, Candidate's Dissertation in Physics and Mathematics (Budker Institute of Nuclear Physics, Siberian Branch, Russian Academy of Sciences, Novosibirsk, 2024).
17. https://nds.iaea.org/.
18. D. Kasatov, I. A. Kolesnikov, A. Koshkarev, A. Makarov, E. Sokolova, I. Shchudlo, and S. Taskaev, J. Instrum. **15**, P10006 (2020). https://doi.org/10.1088/1748-0221/15/10/p10006
19. S. Taskaev, T. Bykov, D. Kasatov, I. Kolesnikov, A. Koshkarev, A. Makarov, S. Savinov, I. Shchudlo, and E. Sokolova, Nucl. Instrum. Methods Phys. Res., Sect. B **502**, 85 (2021). https://doi.org/10.1016/j.nimb.2021.06.010
20. in *Handbook of Stable Isotope Analytical Techniques* (2009), Vol. 2, p. 1123.
21. K. Lieberman, G. J. Alexander, and J. A. Sechzer, Experientia **42**, 985 (1986). https://doi.org/10.1007/bf01940701
22. https://www.nndc.bnl.gov/endf-b8.0/.
23. J. F. Ziegler and J. P. Biersack, *The Stopping and Range of Ions in Matter* (SRIM Company, 2012).

Publisher's Note. Pleiades Publishing remains neutral with regard to jurisdictional claims in published maps and institutional affiliations.

AI tools may have been used in the translation or editing of this article.